Compositional and structural analysis of glycosaminoglycans in cell-derived extracellular matrices

João C. Silva[1,2,4], **Marta S. Carvalho**[1,3,4], **Xiaorui Han**[2], **Ke Xia**[2], **Paiyz E. Mikael**[2], **Joaquim M. S. Cabral**[1,4], **Frederico Castelo Ferreira**[1,4], and **Robert J. Linhardt**[2,3,*]

[1]Department of Bioengineering and iBB - Institute of Bioengineering and Biosciences, Instituto Superior Técnico, Universidade de Lisboa, Av. Rovisco Pais, Lisboa 1049-001, Portugal

[2]Department of Chemistry and Chemical Biology, Biological Sciences and Chemical and Biological Engineering, Center for Biotechnology and Interdisciplinary Studies, Rensselaer Polytechnic Institute, Troy, NY 12180-3590, USA

[3]Department of Biomedical Engineering, Center for Biotechnology and Interdisciplinary Studies, Rensselaer Polytechnic Institute, Troy, NY 12180-3590, USA

[4]The Discoveries Centre for Regenerative and Precision Medicine, Lisbon Campus, Instituto Superior Técnico, Universidade de Lisboa, Av. Rovisco Pais, Lisboa 1049-001, Portugal

Abstract

The extracellular matrix (ECM) is a highly dynamic and complex meshwork of proteins and glycosaminoglycans (GAGs) with a crucial role in tissue homeostasis and organization not only by defining tissue architecture and mechanical properties, but also by providing chemical cues that regulate major biological processes. GAGs are associated with important physiological functions, acting as modulators of signaling pathways regulating several cellular processes such as cell growth and differentiation. Recently, *in vitro* fabricated cell-derived ECM have emerged as promising materials for regenerative medicine due to their ability of better recapitulate the native ECM-like composition and structure, without the limitations of availability and pathogen transfer risks of tissue-derived ECM scaffolds. However, little is known about the molecular and more specifically, GAG composition of these cell-derived ECM. In this study, three different cell-derived ECM were produced *in vitro* and characterized in terms of their GAG content, composition and sulfation patterns using a highly sensitive liquid chromatography-tandem mass spectrometry technique. Distinct GAG compositions and disaccharide sulfation patterns were verified for the different cell-derived ECM. Additionally, the effect of decellularization method on the GAG and disaccharide relative composition was also assessed. In summary, the method presented here offers a novel approach to determine the GAG composition of cell-derived ECM, which we believe is critical for a better understanding of ECM role in directing cellular responses and has the potential for generating important knowledge to use in the development of novel ECM-like biomaterials for tissue engineering applications.

*Corresponding author: linhar@rpi.edu.

Conflict of interest The authors declare no conflict of interest.

Compliance with ethical standards

Ethical approval This work does not contain any studies with human participants or animals performed by any of the authors.

Author Manuscript

Author Manuscript

Author Manuscript

Author Manuscript

Keywords

Glycosaminoglycans; Compositional analysis; Cell-derived extracellular matrix; Disaccharides; Chondrocytes; Mesenchymal stem cells

Introduction

The extracellular matrix (ECM) is a complex and highly specialized three-dimensional meshwork of biomolecules including proteins (e.g., collagen, fibronectin, laminin and others) and proteoglycans. The ECM plays a pivotal role in tissue homeostasis not only by defining tissue architecture and mechanical properties, but also as a modulator of signaling pathways regulating major cellular functions, such as cell proliferation, migration and differentiation [1, 2], Dysregulation of the ECM composition and structure is known to contribute to several pathological conditions, such as fibrosis, cancer and osteoarthritis [3], Due to the importance of its functions and the versatility of its native tissue-like properties, ECM obtained from the decellularization of tissues has been widely used as bioactive scaffolds for several tissue engineering and regenerative medicine applications [4, 5], However, the scarcity of autologous organs/tissues and the occurrence of immunogenic responses and pathogen transfer when allogeneic/xenogeneic sources were used limited the clinical use of whole organ/tissue-derived decellularized ECM [6], An alternative approach to overcome these limitations, the use of cultured cells to generate ECM decellularized scaffolds *in vitro* has been recently explored. Cell-derived ECM present additional advantages over tissue-derived ECM such as they can mimic the composition of native ECM that is hard to isolate from tissues (e.g., stem cell niche) and they can be used to modify the surface of synthetic/natural biomaterial scaffolds, generating constructs with improved bioactivity and appropriate mechanical support [1, 7–9], Additionally, as ECM compositions vary considerably with cell type and tissue location, cell source selection is a crucial factor for the success of the tissue engineering strategy.

Mesenchymal stem cells (MSC) have been employed as one of the major sources to generate cell-derived ECM scaffolds for regenerative medicine applications, mainly targeting bone and cartilage repair [1, 10–12], MSC are adult multipotent cells with a high *in vitro* expansion capability and able to differentiate into bone, cartilage and adipose tissue. Additionally, these cells are readily available as they can be isolated from several tissues including bone marrow, fat, umbilical cord matrix and synovium, and possess advantageous properties that favor a regenerative microenvironment such as low-immunogenicity and trophic/immunomodulatory activity [13, 14], Regarding cartilage repair strategies, chondrocytes, unique cell population present in cartilage tissue, have also been successfully used to generate cell-derived ECM scaffolds [15, 16], However, despite all these studies, little is currently known about the molecular composition of *in vitro* produced cell-derived ECM, namely in terms of the specific types and amounts of proteins and proteoglycans retained after the decellularization process.

Proteoglycans are major structural components of ECM and consist of a core protein with one or more covalently attached glycosaminoglycan (GAG) chains. Proteoglycans are able

to bind to many growth factors, cytokines and chemokines, which make them key modulators of cellular functions and tissue development [17, 18], GAGs are a family of linear, negatively charged carbohydrates with a repeating disaccharide unit. Based on the structure and sulfation level of the repeating disaccharide, GAGs can be generally classified into four families that include heparan sulfate (HS), chondroitin sulfate (CS), keratan sulfate (KS) and hyaluronic acid (HA) [18, 19], Proteoglycans and respective GAGs localize mainly in cell membranes and reside within the ECM, acting as molecular co-receptors in cell signaling for cell-cell and cell-ECM interactions important for cell survival and differentiation [18], The negatively charged GAGs are also associated with the maintenance of the biomechanical properties of tissues through controlling of hydration and swelling pressure, allowing tissues to absorb compressional forces. Additionally, the sulfation patterns in the GAG chains play crucial roles by allowing interactions, mainly of an ionic nature, with growth factors, cell surface receptors, enzymes, cytokines, chemokines and proteins that are associated with several biological processes, such as development, disease, cell growth and differentiation and microbial pathogenesis[20–23]. In fact, GAGs role in controlling stem cell fate through modulation of important signaling pathways such as FGF signaling was previously suggested [18, 21, 24], Additionally, the effects of different GAGs in MSC proliferation and differentiation through mediation of growth factor activity have also been reported in the literature [25–28], Therefore, the structural and growth factor sequestering/activation properties of GAGs make these biomolecules promising materials for a broad range of tissue engineering applications [19, 20, 29], As major components of cartilage, GAGs, mainly CS and HA, have been incorporated in tissue engineering scaffolds to more effectively mimic the natural ECM and improve the quality of the generated tissue [30–32].

As a result of critical importance of GAGs in regulating many physiological processes in all organisms, accurately determining their composition, structure and sulfation patterns as well as their changes in normal versus diseased states in different organs, tissues, and cells is necessary to better understand the underlying mechanisms involved in normal development and several pathologies. Recently studies have been conducted to elucidate the "GAGome" and glycome changes related to specific cellular functions and diseases. Our group previously reported differences in GAG sulfation patterns between cancerous and normal tissues as well between lethal and nonlethal breast cancer tissues [33], Glycomics of MSC was previously suggested as a valuable tool to evaluate their differentiation stage [34], Moreover, high performance liquid chromatography (HPLC) analysis combined with mass spectrometry has been used to study GAGs as possible markers of MSC differentiation potential [35], Despite the availability of many different qualitative and quantitative techniques for analyzing GAGs, liquid chromatography-tandem mass spectrometry (LC-MS/MS) method using multiple reaction monitoring (MRM) detection represents a major advancement in the field of glycosaminoglycanomics due to its high sensitivity and specificity for detecting all GAG subtypes in complex biological samples [36, 37], This method has been successfully applied, by our group and others, to analyze GAG disaccharides in various types of samples including biological fluids (e.g., plasma and urine) [37, 38], human milk at different lactation stages [39], cultured cells [40] and different regions of human intervertebral disc [41], Interestingly, despite the great promise and

attention received by tissue engineering and regenerative medicine research, only few studies have employed proteomics and glycomics methods to provide more complete molecular characterization of decellularized ECM scaffolds or final engineered tissues.

In the present study, cell-derived ECM from different cell sources were generated and characterized qualitatively in terms of the efficacy of the decellularization process, their morphology and presence of relevant ECM proteins. Additionally, after GAG extraction, purification and enzymatic digestion, we used LC-MS/MS with MRM detection mode to perform GAG disaccharide compositional analysis of *in vitro* produced cell-derived ECM and respective cell sources. A workflow diagram of the procedures used to determine GAG content and composition of the different cells and cell-derived ECM samples is presented in Fig. 1. These analyses can generate relevant knowledge about the GAG content and composition of the ECM secreted by these cells, which may provide new insights for the design of novel ECM biomimetic biomaterial scaffolds for regenerative medicine applications, especially for cartilage repair. Additionally, these results can also provide some understanding of how GAG composition, structure and sulfation levels are affected by the decellularization method used.

Materials and methods

Cell culture

Human chondrocytes purchased from CELL Applications, Inc. were cultured using high-glucose Dulbecco's Modified Eagle's Medium (DMEM: Gibco, Grand Island NY, USA) supplemented with 10% fetal bovine serum (FBS: Gibco, USA), IX MEM non-essential aminoacids (Sigma, St. Louis MO, USA), 0.2 mM L-Ascorbic acid (Sigma), 0.4 mM L-Proline (Sigma) and 1% penicillin-streptomycin (Pen-strep: Gibco). Human bone marrow MSC (BMSC, male 36 years) and human synovial MSC (SMSC, male 28 years) were isolated according to protocols previously established [42, 43]. Bone marrow aspirates were obtained from Instituto Português de Oncologia Francisco Gentil, Lisboa-Potugal while synovium aspirates were obtained from Centro Hospitalar de Lisboa Ocidental, E.P.E, Hospital São Francisco Xavier, Lisboa, Portugal. All human samples were obtained from healthy donors after written informed consent according to the Directive 2004/23/EC of the European Parliament and of the Council of 31 March 2004 on setting standards of quality and safety for the donation, procurement, testing, processing, preservation, storage and distribution of human tissues and cells (Portuguese Law 22/2007), with the approval of the Ethics Committee of the respective clinical institution. Isolated BMSC and SMSC were cultured using DMEM supplemented with 10% FBS and 1% Pen-strep and cryopreserved in liquid/vapour nitrogen tanks until further use. All cultures were kept at 37 °C and 5% CO_2 in a humidified atmosphere and only cells between passages 3 and 5 were used in this study.

Materials

Unsaturated disaccharide standards of CS, HS and HA were purchased from Iduron (Manchester, UK., see Table 1 for structures). Sodium cyanoborohydrade ($NaCNBH_4$), 2-aminoacridone (AMAC) and acetic acid were obtained from Sigma-Aldrich (St. Louis MO, USA). Methanol (HPLC grade), water (HPLC grade), ammonium acetate (HPLC grade) and

dimethyl sulfoxide (DMSO) were purchased from Fisher Scientific (Springfield NJ, USA). Enzymes chondroitin lyase ABC from *Proteus vulgaris* and recombinant *Flavobacterial* heparinase I, II and III were expressed in *E. coli* strains in our laboratory.

Decellularized cell-derived ECM preparation

Human chondrocytes, BMSC and SMSC were seeded in tissue culture-treated plates at 5000 cells/cm^2 and expanded in their respective media (see Materials and methods-Cell culture subsection) for 10-12 days with complete medium renewal twice a week. After reaching confluency, medium was discarded and cells were washed in Dulbecco's phosphate buffered saline (PBS, no calcium, no magnesium - catalog# 14190144, Gibco). ECM isolation was performed by a decellularization protocol using a 20 mM ammonium hydroxide (NH$_4$OH, Sigma) + 0.5% Triton X-100 (Sigma) solution in PBS according to previously reported methods [9, 11]. The solution was added to the culture and incubated for 5 min at room temperature. After confirmation of complete cell lysis and presence of intact ECM on the surface of the wells under a microscope, ECM was gently washed 3 times with distilled water. Then, the different cell-derived ECM layers were detached from the plates using a cell scrapper, collected in falcon tubes and freeze-dried. Cell culture monolayers before decellularization were washed twice with PBS to remove any media remnants, harvested and the pellets were collected by centrifugation. Afterwards, the cell pellets were rinsed twice with PBS, centrifuged and collected for GAG disaccharide analysis.

Immunofluorescence analysis

The success of the decellularization protocol for the different cell sources was confirmed by immunocytochemistry and phase/fluorescence microscopy. Therefore, cultures before and after decellularization were washed twice with PBS, fixed with 4% paraformaldehyde (PFA; Santa Cruz Biotechnology, Dallas TX, USA) for 30 min and then permeabilized with 0.1% Triton X-100 for 10 min. After permeabilization, samples were incubated with phalloidin-TRITC (Sigma-Aldrich) (dilution 1:250, 2 μg/mL) for 45 min in the dark. Then, cells were washed twice with PBS and counterstained with DAPI (Sigma-Aldrich) (1.5 μg/mL) for 5 min and then washed with PBS. Cell cultures before and after decellularization were imaged in phase contrast mode and fluorescent mode under a microscope (Olympus IX51 Inverted Microscope: Olympus America Inc., Melville NY, USA).

The presence and distribution of the ECM proteins collagen I, fibronectin and laminin in the different cell-derived ECM was assessed by immunofluorescence staining. After decellularization, samples were washed with PBS and fixed with 4% PFA for 30 min at room temperature. Afterwards, cell-derived ECM were washed three times with 1% bovine serum albumin (BSA, Sigma) in PBS for 5 min. Cell-derived ECM were then blocked with a solution of 1% BSA and 10% donkey serum (Sigma) in PBS at room temperature for 45 min. Primary antibodies including mouse anti-human collagen I, fibronectin and laminin (10 μg/ml in 1% BSA, 10% donkey serum in PBS) (R&D systems, Minneapolis, MN) were added into the samples, followed by an overnight incubation at 4°C. After washing with 1% BSA in PBS, a NorthemLights™ 557-conjugated anti-sheep IgG secondary antibody (dilution 1:200 in 1%BSA PBS solution) (R&D systems) was added into the samples and incubated in the dark for 1 h at room temperature. Cell nuclei were counterstained with

DAPI (1.5 μg/ml) for 5 min and the samples were finally washed with PBS to further confirm complete decellularization. Immunofluorescence staining was confirmed by microscopy (Olympus IX51 Inverted Microscope).

Scanning electron microscopy analysis

The morphological analysis of the different cell-derived ECM was performed using a field emission scanning electron microscope (FE-SEM, FEI-Versa 3D Dual Beam, Hillsboro). Before imaging, cell-derived ECM samples obtained in glass cover slips were mounted on a holder and sputter-coated with a thin layer of 60% gold-40% palladium. SEM imaging was performed at different magnifications using an accelerating voltage of 2 kV.

GAG disaccharide sample preparation: isolation, digestion and AMAC-labeling

Cell confluent monolayers and respective lyophilized cell-derived ECM samples collected from one culture dish were treated with 100 μL of BugBuster 10× Protein Extraction Reagent (Millipore Sigma, MA USA) and sonicated for 1 h. The samples were then desalted by passing through a 3 KDa molecular weight cut off (MWCO) spin column (Millipore, MA USA), and washed three times with distilled water. The casing tubes were replaced and 300 μL of digestion buffer (50 mM ammonium acetate containing 2 mM calcium chloride adjusted to pH 7.0) was added to the filter unit. Afterwards, recombinant heparin lyases I, II, III (10 mU each, pH optima 7.0–7.5) and recombinant chondroitin lyase ABC (10 mU each, pH optimum 7.4) were added to each sample, mixed well by pipetting and samples GAG enzymatic digestion was conducted by incubation overnight at 37 °C. The enzymatic reaction was terminated by centrifugal ultrafiltration, the disaccharides were recovered in the filtrate and the fdter unit was washed twice with 200 μL of distilled water. The final fdtrates containing the disaccharide products were lyophilized and kept at −20 °C until labeling.

Dried cell and cell-derived ECM disaccharide samples were AMAC-labeled by adding 10 μL of 0.1M AMAC in DMSO/acetic acid (17/3, V/V) solution by incubating at room temperature for 10 min, followed by addition of 10 μL of 1M aqueous $NaCNBH_4$ solution and incubation for 1 h at 45 °C. A mixture containing all 17 CS, HS and HA disaccharide standards (derivatives of the structures shown in Fig. 1 are summarized in Table 1) prepared at a concentration of 0.5 ng/μL was similarly AMAC-labeled (structures in Supplementary Figure 2) and used for each ran as an external standard. After the AMAC-labeling reaction, the samples were centrifuged and respective supernatants were recovered.

Compositional analysis of GAG disaccharides by LC-MS/MS

Disaccharide analysis was performed according to a previously reported method [37]. LC was performed on an Agilent 1200 LC system at 45 °C using an Agilent Poroshell 120 ECC18 (2.7 μm, 3.0 × 50 mm) column. Mobile phase A (MPA) was 50 mM ammonium acetate aqueous solution, and the mobile phase B (MPB) was methanol. The mobile phase passed through the column at a flow rate of 300 μL/min. The gradient used was the following: 0-10 min, 5-45% B; 10-10.2 min, 45-100% B; 10.2-14 min, 100% B; 14-22 min, 100-5% B. The injection volume used for all the samples was 5 μL.

A triple quadrupole mass spectrometry system equipped with an ESI source (Thermo Fisher Scientific, San Jose CA, USA) was used a detector. The online MS analysis was performed at the Multiple Reaction Monitoring (MRM) mode with the MS parameters: negative ionization mode with a spray voltage of 3000 V, a vaporizer temperature of 300 °C, and a capillary temperature of 270 °C. Data analysis was performed using Thermo Xcalibur™ software (Thermo Fisher Scientific, San Jose CA, USA). The disaccharides in different cell and cell-derived ECM samples were quantified by comparison of the sample peak area to that of an external standard.

Statistical analysis

All values were represented as the mean ± standard deviation (SD) of 3 independent samples. Statistical analysis of the data was performed using the software GraphPad Prism version 7. One-way analysis of variance (ANOVA) was performed to determine significant differences among the multiple groups of data of cell-derived ECM and cell culture monolayers. Tukey's post-hoc test was used to determine the difference between any two groups. Student's t-test was used to determine significant differences in each GAG disaccharide composition between cell-derived ECM and respective cell culture before decellularization. Data were considered statistically significant if $p < 0.05$.

Results

Cell-derived ECM characterization

Decellularized cultured cell-derived ECM was obtained from three different human cell types (chondrocytes, BMSC and SMSC). Cultures were fully confluent before decellularization and presented a spindle-like morphology, characteristic of these cell types, with a well defined cell nuclei and cytoskeleton, as it is possible to observe in the fluorescent micrographs obtained after DAPI/Phalloidin staining (Fig. 2). After the decellularization treatment with a solution of 20 mM NH_4OH and 0.5% Triton X-100 in PBS for 5 min, it is possible to confirm the presence of a fibrillary network of ECM in all the different conditions. The residual DAPI staining after decellularization indicated that the cellular nuclei were disrupted and only the ECM secreted by cells remained, therefore confirming the success of the decellularization method used (Fig. 2).

The quality of the cell-derived ECM was assessed by immunostaining for the presence of known relevant ECM proteins, namely collagen type I, fibronectin and laminin. After decellularization, all the conditions stained positively for ECM proteins collagen type I, fibronectin and laminin (Fig. 3). However, some differences in ECM proteins relative abundance were observed between the different cell-derived ECM. Accordingly, Fig. 3 results shows that SMSC-ECM presented a considerably lower level of fluorescent staining for all the proteins when compared with BMSC-ECM. Additionally, BMSC-ECM apparently expressed higher levels of collagen I, fibronectin and laminin than the other two types of cell-derived ECM studied.

The morphology and micro/nano scale features of the different cell-derived ECM were assessed by SEM analysis (Fig. 4). All the cell-derived ECM types presented a similar

architecture composed by fibrillar networks. However, for the case of SMSC-ECM, as we can observe in Fig. 4, it was also possible to identify some globular-like structures together with fibrillar ones.

Disaccharide composition of cell-derived ECM

The total amount of GAG (Fig. 5a and Supplementary Table 1) as well as the respective HS, CS and HA GAG amounts (Fig. 5b and Supplementary Table 1) for each cell-derived ECM were obtained after LC-MS/MS analysis and normalized to the dry weight of each sample. As it is possible to observe in Fig. 5a, BMSC-ECM contained significant higher amounts of total GAG than Chondrocyte-ECM and SMSC-ECM. Regarding HS, CS and HA total composition (expressed as ng of GAG/mg of dry cell-derived ECM), there were evident differences in the GAG compositions of the cell-derived ECM obtained from different cell sources (Fig. 5b). Chondrocyte-ECM was composed mainly by CS (86 ± 36 ng/mg), followed by lower average amounts of HS (16 ± 4 ng/mg) and HA (10 ± 6 ng/mg). Both BMSC-ECM (HA: 88 ± 20 ng/mg; CS: 79 ± 23 ng/mg; HS: 39 ± 16 ng/mg) and SMSC-ECM (CS: 35 ± 2 ng/mg; HA: 32 ± 8 ng/mg; HS: 8 ± 1 ng/mg) were more evenly composed by CS and HA, with lower amounts of HS. Interestingly, BMSC-ECM presented significantly higher amounts of HA when compared to ECM secreted by the other cell types.

The compositional analysis of the GAG disaccharides of the different cell-derived ECM was performed after enzymatic digestion of isolated GAG samples with heparin lyase I, II, III and chondroitin lyase ABC. The disaccharides were then AMAC-labeled by reductive amination and analyzed by LC-MS/MS using MRM. The HS and CS disaccharide composition for the different cell-derived ECM normalized to dry ECM weight is presented in Fig. 6 and Supplementary Table 2. For all the cell-derived ECM, HS was comprised primarily of 0S, followed by NS and N2S (Fig. 6a). However, some differences were noticed in the HS disaccharide amounts present in the different types of ECM. BMSC-ECM presented a significantly higher amount of 0S and NS when compared to SMSC-ECM and Chondrocyte-ECM. Additionally, Chondrocyte-ECM presented a statistically significant higher amount of NS2S than the ECM derived from both MSC sources. In terms of CS disaccharides, all the cell-derived ECM conditions were primarily composed by 4S and 6S (Fig. 6b). The amounts of 4S were significantly higher in BMSC-ECM comparing to other conditions of cell-derived ECM. Moreover, Chondrocyte-ECM presented higher amounts of 6S, however the difference was only statistically significant when compared to SMSC-ECM.

Effects of the decellularization process on GAG amount and disaccharide percentage composition

The effect of the decellularization protocol on the total GAG amount of the different cell types tested was evaluated by quantifying the mass of GAG recovered from each culture dish before and after the treatment (Fig. 7a and 7b, Supplementary Table 3). BMSC presented a significantly higher total GAG amount compared to the other cell types. Additionally, as expected, the amounts of total GAG per dish were considerably lower in the cell-derived ECM samples comparing to the cell monolayers. However, the amounts of total GAG retained for the different types of cell-derived ECM were moderately close (Chondrocyte-ECM: 200 ± 78 ng/dish; BMSC-ECM: 223 ± 48 ng/dish; SMSC-ECM: 134 ± 17 ng/dish),

with percentages of GAG retention varying between 20-30%. In Fig. 7b and Supplementary Table 3, it is possible to observe the amounts of HS, CS and HA recovered from each culture dish for the different cell-derived ECM and respective monolayer cultures. As it is possible to observe, the decellularization process differentially affected HS, CS and HA GAG amounts among the different cultures. For example, CS was significantly lost during the generation of Chondrocyte-ECM and SMSC-ECM, which was not verified for BMSC-ECM. Contrarily, percentage-wise, HA was greatly diminished during BMSC decellularization, while approximately maintained during the generation of SMSC-ECM. This differential response was also observed for the HS and CS disaccharide amounts before and after decellularization, which are summarized in the Supplementary Table 4.

The average GAG disaccharide percentage compositions of the various cell-derived ECM were determined and compared to the respective culture monolayers to further assess the effect of the decellularization method on GAG amount, sulfation level and disaccharide composition. The average HS, CS and HA percentage composition of the different cell-derived ECM and respective cell sources before decellularization is presented in Fig. 7c and Supplementary Table 5. All the cell-derived ECM presented significantly different HS, CS and HA percentage compositions when compared to its respective cell source, with the exception of HS percentage composition of SMSC-ECM and SMSC. Cultured chondrocytes were mainly composed by CS (50%), followed by HS (31%) and HA (19%). After decellularization, the generated Chondrocyte-ECM contained a higher relative average percentage of CS (77%) and lower relative average percentages of HS (15%) and HA (9%) when compared to chondrocyte cells. BMSC GAGs are mainly composed of HA (80%) with relatively low average percentages of HS (10%) and CS (10%). However, the ECM generated from BMSC consisted of a completely different GAG composition, with similar percentages of HA (43%) and CS (38%), but a lower percentage of HS (18%). SMSC cultures GAG mixtures were mainly composed of CS (68%), and lower relative percentages of HA (19%) and HS (13%). SMSC-ECM showed a lower percentage of CS (47%), a higher percentage of HA (42%) and a slightly lower percentage of HS (10%). Despite the differences verified for the cell monolayers, the average percentage compositions of matrices generated from two different MSC sources, BMSC-ECM and SMSC-ECM, were fairly similar (HS: 18% vs. 10%; CS: 38% vs. 47% and HA: 43% vs. 42%, respectively).

The differences in average percentage HS and CS disaccharide composition between cultured cells and *in vitro* fabricated cell-derived ECM were also assessed and are presented in Fig. 8 and Supplementary Table 6. Chondrocytes and Chondrocyte-ECM HS were mainly composed by 0S, NS and NS2S with significant differences observed after decellularization (Fig. 8a), namely a relatively lower average percentage of 0S and relatively higher average percentages of NS2S and NS in Chondrocyte-ECM when compared to chondrocyte cells. In terms of CS disaccharides (Fig. 8b), Chondrocyte-ECM was mainly composed of 6S (63%), 4S (27%) and 0S (7%), and these values are significantly different from the observed values for CS composition of chondrocyte cells, which were composed of 4S (76%), and a lower percentage of 6S (17%) and a very small percentage of 0S (1%). BMSC-ECM HS was primarily composed of 0S (65%) and NS (28%) with low percentage of NS2S (4%), whereas the HS composition observed for BMSC cell cultures was 0S (57%) and NS (27%) and NS2S (16%). Both BMSC cultured cells and BMSC-ECM showed CS disaccharide

compositions predominantly composed of 4S and 6S. However, significant differences were observed, with BMSC-ECM having a lower average percentage of 4S (55% vs. 75%) and a higher average percentage of 6S (41% versus 18%), compared to cultured cells. HS from both SMSC cultured cells and SMSC-ECM was mainly composed of 0S (72% and 68%, respectively) with lower average percentages of NS and NS2S. Interestingly, significant differences in HS disaccharide composition between SMSC-ECM and their respective cell source were observed only for NS2S and a low percentage of 2S (6%) was detected in the cultured cells. The CS disaccharide compositions were similar to the observed for the other cell types, with both SMSC cultures and SMSC-ECM mainly composed of 4S and 6S. Additionally, the same trend was observed with SMSC-ECM, which showed a significantly lower percentage of 4S (56% versus 71%) and a significantly higher percentage of 6S (38% versus 21%) when compared to SMSC cell cultures before decellularization treatment.

Discussion

In this study, we produced different cell-derived ECM secreted from human chondrocytes, BMSC and SMSC based on previously reported methods [9, 11]. Fluorescent microscopy and DAPI/phalloidin staining were used to observe cell cultures before and after decellularization and confirm the efficiency of the method. All cells were removed and a fibrillary network of ECM was observed for all conditions. Moreover, the different cell-derived ECM samples produced were also characterized for the presence of ECM proteins (collagen I, fibronectin and laminin). After removal of cellular components, these ECM proteins were still present as constituents of the cell-derived ECM. However, differences in the protein abundance and distribution were observed among the ECM-derived from different cell sources. Despite evidences of the presence of ECM proteins, a lower level of fluorescent staining was observed for all proteins in SMSC-ECM. However, this is accordance with the phase microscopy images from Fig.2, in which a considerably lower amount of ECM network was obtained for SMSC-ECM when compared to Chondrocyte-ECM and BMSC-ECM. BMSC-ECM produced in this work stained positive for all the 3 ECM proteins, with lower staining area verified for laminin, which is in accordance to a previously published study [8]. These BMSC-ECM characterization results were consistent with a previous study that has shown the retention of ECM proteins after complete decellularization of adipose tissue derived-MSC *in vitro* cultures[44]. Concerning Chondrocyte-ECM, both fibronectin and collagen I presented higher levels of positive fluorescent staining than laminin. The presence of collagen I in the ECM was expected due to fact that chondrocytes tend to increase the expression of this protein when cultured as monolayer plastic adherent cultures. Previous literature also obtained similar results after immunofluorescence analysis of ECM secreted by human articular chondrocytes[45]. The morphology of the different cell-derived ECM was also characterized using SEM and a fibrillar structure was mainly observed, which was consistent with recently published reports [46, 47].

Proteoglycans and their major constituents, GAGs, are among the most important components of the ECM of multiple tissues. GAGs are associated with important physiological functions in maintaining tissue homeostasis and structure and also as modulators of signaling pathways regulating cellular processes. Despite the great importance

of GAGs within the ECM and the increasing number of studies targeting tissues and cells, few studies have focused on the GAGome profile of only ECM. However, recently, authors have been focused on studying the ECM proteome, or as recently defined as "matrisome" of healthy and disease tissues, aiming to identify novel prognostic/diagnostic markers and discover novel therapeutic opportunities [2]. Additionally, other groups have applied proteomic tools to perform a comprehensive characterization of the protein composition of cell-derived ECM produced *in vitro* by BMSC, adipose-derived MSC and neonatal fibroblasts [47]. We assert that the characterization of the GAG content, composition and sulfation patterns of *in vitro* produced cell-derived ECM is critical for a better comprehension of ECM role in directing cellular responses, with the potential of generating useful information to improve the design of novel biomaterials that better recapitulate ECM signaling for tissue engineering and regenerative medicine applications.

In this study, we used a previously developed method of LC-MS/MS with MRM [37] to characterize *in vitro* cell-derived ECM obtained from human chondrocytes, BMSC and SMSC in terms of their GAG content, composition and sulfation pattern. By comparative analysis with the respective cell culture monolayers it was also possible to assess the effects of the decellularization protocol on total GAG and GAG disaccharide amounts. About 20-30% of the GAG amount verified in the cell monolayers cultures was maintained after generation of the different cell-derived ECM. A higher percentage of GAG retention after decellularization (approximately 50%) was obtained in a previous study with adipose stem cell-derived ECM [44]. However, the method used for total GAG quantification was considerably less sensitive than the LC-MS/MS MRM used in this work. Importantly, HS, CS and HA and their disaccharides in the different conditions of cell-derived ECM were differently affected by the decellularization treatment. However a statistically significant loss of HS was verified for all the groups during the decellularization, which might be explained by the depletion of cell surface HS proteoglycans during cell membrane disruption.

Chondrocyte-ECM was mainly consisted of CS and showed higher amounts and relative percentages of this GAG than both BMSC-ECM and SMSC-ECM. Chondrocytes are a unique native cell population within articular cartilage tissue and are responsible for secreting articular cartilage ECM. In articular cartilage, the predominant proteoglycan is aggrecan that consists of a core protein mainly with attached CS chains but also KS chains and small amount of dermatan sulfate (DS) chains [48, 49]. Since the main function of chondrocyte is to secrete cartilage ECM, it is expected that they would synthesize a matrix richer in CS when compared to other cell types, which is consistent with our results. Interestingly, it was previously reported that the chondrocyte proteoglycan metabolism can be directly or indirectly influenced by the scaffold material, as different synthetic and natural materials seeded with chondrocytes resulted in differences in GAG composition and CS sulfation [50]. ECM composition and therefore also GAG composition is known to be dependent on the cell source [47]. Each cell type secretes unique and specific ECM to fulfill the biological requirements of its native tissue. Here, we observed a similarity in GAG composition and HS, CS disaccharide compositions between BMSC-ECM and SMSC-ECM than when these are compared to Chondrocyte-ECM. This suggests that despite being isolated from different tissues, both BMSC and SMSC secrete a more similar ECM in terms of GAG composition when compared to chondrocytes. The HS of cell-derived ECM were

mainly composed of 0S with low amounts of NS and NS2S, whereas the CS of cell-derived ECM consisted of 4S and 6S. Different trends in CS 4S and 6S were observed for MSC-derived ECM and Chondrocyte-ECM. BMSC-ECM and SMSC-ECM showed slightly higher average relative percentages of 4S than 6S, while Chondrocyte-ECM showed a considerably higher average relative percentage of 6S than 4S. It is well established that the disaccharide composition of CS varies with age and degeneration of articular cartilage [51]. Accordingly, during embryogenesis CS chains are exclusively 6S, from fetal development to adolescence CS chains tend to be equally 4S and 6S, and during adulthood CS chains tend to have more 6S than 4S [50, 52]. We speculate that the more "immature" state of BMSC and SMSC and their known involvement in cartilage development, might prime them to secrete a more "juvenile-like" ECM with higher CS4S relative percentages when compared to the ECM secreted by adult chondrocytes. However, additional and more comprehensive studies are required to understand if the known relation of 4S and 6S in articular cartilage tissue can be expanded to cultured cells and cell-derived ECM.

After comparison between the different cell-derived ECM and their respective cultured cells before decellularization, we observed significant differences on the relative average percentages of total GAGs and HS and CS disaccharides. Despite the differences in the relative average percentages, the trends observed in the CS disaccharides changes after the decellularization process were similar among the different samples, more specifically, all the cell-derived ECM samples showed lower relative average percentages of 4S and higher relative average of percentages of 6S when compared to the cultured cells before decellularization. Such similarities among the different conditions were not so clearly observed for HS disaccharides.

In summary, we successfully fabricated cell-derived ECM from different cell sources and characterized them in terms of their morphology and presence of relevant ECM proteins. Moreover, a highly sensitive and specific LC-MS/MS analytical method was used for the first time to determine the GAG content, composition and sulfation patterns of *in vitro* generated cell-derived ECM. Significant differences in GAG composition were observed between the cell-derived ECM secreted by different cell sources, confirming the expected tissue-ECM specificity. Finally, the analytical method presented in this first report of GAG composition of cell-derived ECM, together with further studies combining proteomic tools, might provide important knowledge to better understand ECM molecular composition and function in regulating cellular responses. The structure-function studies should further the development of improved ECM-like biomimetic scaffolds for tissue engineering applications.

Supplementary Material

Refer to Web version on PubMed Central for supplementary material.

Acknowledgments

References

1. Lu H, Hoshiba T, Kawazoe N, Koda I, Song M, Chen G: Cultured cell-derived extracellular matrix scaffolds for tissue engineering. Biomaterials. 32, 9658–9666 (2011). doi: 10.1016/j.biomaterials.2011.08.091 [PubMed: 21937104]

2. Naba A, Clauser KR, Ding H, Whittaker CA, Carr SA, Hynes RO: The extracellular matrix: Tools and insights for the "omics" era. Matrix Biol. 49, 10–24 (2016). doi:10.1016/j.matbio.2015.06.003 [PubMed: 26163349]

3. Bonnans C, Chou J, Werb Z: Remodelling the extracellular matrix in development and disease. Nat. Rev. Mol. Cell Biol 15, 786–801 (2014). doi: 10.1038/nrm3904 [PubMed: 25415508]

4. Gilbert TW, Sellaro TL, Badylak SF: Decellularization of tissues and organs. Biomaterials. 27, 3675–3683 (2006). doi: 10.1016/j.biomaterials.2006.02.014 [PubMed: 16519932]

5. Badylak SF, Taylor D, Uygun K: Whole Organ Tissue Engineering: Decellularization and Recellularization of Three-Dimensional Matrix Scaffolds Annu. Rev. Biomed. Eng 13, 27–53 (2010). doi:10.1146/annurev-bioeng-071910-124743

6. Wong ML, Griffiths LG: Immunogenicity in xenogeneic scaffold generation: Antigen removal vs. decellularization. Acta Biomater. 10, 1806–1816 (2014). doi:10.1016/j.actbio.2014.01.028 [PubMed: 24486910]

7. Hoshiba T, Lu H, Kawazoe N, Chen G: Decellularized matrices for tissue engineering. Expert Opin. Biol. Ther 10, 1717–1728 (2010). doi: 10.1517/14712598.2010.534079 [PubMed: 21058932]

8. Lu H, Hoshiba T, Kawazoe N, Chen G: Autologous extracellular matrix scaffolds for tissue engineering. Biomaterials. 32, 2489–2499 (2011). doi: 10.1016/j.biomaterials.2010.12.016 [PubMed: 21211834]

9. Kang Y, Kim S, Bishop J, Khademhosseini A, Yang Y: The osteogenic differentiation of human bone marrow MSCs on HUVEC-derived ECM and β-TCP scaffold. Biomaterials. 33, 6998–7007 (2012). doi: 10.1016/j.biomaterials.2012.06.061 [PubMed: 22795852]

10. Zeitouni S, Krause U, Clough BH, Halderman H, Falster A, Blalock DT, Chaput CD, Sampson HW, Gregory CA: Human mesenchymal stem cell-derived matrices for enhanced osteoregeneration. Sci. Transl. Med. 4, 132–155 (2012). doi:10.1126/scitranslmed.3003396

11. Yang Y, Lin H, Shen H, Wang B, Lei G, Tuan RS: Mesenchymal stem cell-derived extracellular matrix enhances chondrogenic phenotype of and cartilage formation by encapsulated chondrocytes in vitro and in vivo. Acta Biomater. 69, 71–82 (2018). doi: 10.1016/j.actbio.2017.12.043 [PubMed: 29317369]

12. Zhang W, Zhu Y, Li J, Guo Q, Peng J, Liu S, Yang J, Wang Y: Cell-Derived Extracellular Matrix: Basic Characteristics and Current Applications in Orthopedic Tissue Engineering. Tissue Eng. Part B Rev. 22, 193–207 (2016). doi: 10.1089/ten.teb.2015.0290 [PubMed: 26671674]

13. Dominici M, Le Blanc K, Mueller I, Slaper-Cortenbach I, Marini FC, Krause DS, Deans RJ, Keating A, Prockop DJ, Horwitz EM: Minimal criteria for defining multipotent mesenchymal stromal cells. The International Society for Cellular Therapy position statement. Cytotherapy. 8, 315–317 (2006). doi: 10.1080/14653240600855905 [PubMed: 16923606]

14. Murphy MB, Moncivais K, Caplan AI: Mesenchymal stem cells: Environmentally responsive therapeutics for regenerative medicine, (2013)

15. Jin CZ, Choi BH, Park SR, Min BH: Cartilage engineering using cell-derived extracellular matrix scaffold in vitro. J. Biomed. Mater. Res. - Part A. 92, 1567–1577 (2010). doi:10.1002/jbm.a.32419

16. Park YB, Seo S, Kim JA, Heo JC, Lim YC, Ha CW: Effect of chondrocyte-derived early extracellular matrix on chondrogenesis of placenta-derived mesenchymal stem cells. Biomed. Mater. 10, (2015). doi: 10.1088/1748-6041/10/3/035014

17. Linhardt RJ, Toida T: Role of glycosaminoglycans in cellular communication. Acc. Chem. Res. 37, 431–438 (2004). doi:10.1021/ar030138x [PubMed: 15260505]

18. Gasimli L, Linhardt RJ, Dordick JS: Proteoglycans in stem cells. Biotechnol. Appl. Biochem. 59, 65–76 (2012). doi:10.1002/bab.1002 [PubMed: 23586787]

19. Weyers A, Linhardt RJ: Neoproteoglycans in tissue engineering. FEBS J. 280, 2511–2522 (2013). doi: 10.1111/febs.12187 [PubMed: 23399318]

20. Wang M, Liu X, Lyu Z, Gu H, Li D, Chen H: Glycosaminoglycans (GAGs) and GAG mimetics regulate the behavior of stem cell differentiation. Colloids Surfaces B Biointerfaces. 150, 175–182 (2017). doi: 10.1016/j.colsurfb.2016.11.022 [PubMed: 27914254]

21. Papy-Garcia D, Albanese P: Heparan sulfate proteoglycans as key regulators of the mesenchymal niche of hematopoietic stem cells. Glycoconj. J 34, 377–391 (2017). doi:10.1007/s10719-017-9773-8 [PubMed: 28577070]

22. Gasimli L, Hickey AM, Yang B, Li G, Dela Rosa M, Nairn AV, Kulik MJ, Dordick JS, Moremen KW, Dalton S, Linhardt RJ: Changes in glycosaminoglycan structure on differentiation of human embryonic stem cells towards mesoderm and endoderm lineages. Biochim. Biophys. Acta - Gen. Subj 1840, 1993–2003 (2014). doi:10.1016/j.bbagen.2014.01.007

23. Kjellén L, Lindahl U: Specificity of glycosaminoglycan–protein interactions. Curr. Opin. Struct. Biol. 50, 101–108 (2018). doi: 10.1016/j.sbi.2017.12.011 [PubMed: 29455055]

24. Ibrahimi OA, Zhang F, Hrstka SCL, Mohammadi M, Linhardt RJ: Kinetic Model for FGF, FGFR, and Proteoglycan Signal Transduction Complex Assembly. Biochemistry. 43, 4724–4730 (2004). doi: 10.1021/bi0352320 [PubMed: 15096041]

25. Cool SM, Nurcombe V: The osteoblast-heparan sulfate axis: Control of the bone cell lineage. Int. J. Biochem. Cell Biol. 37, 1739–1745 (2005). doi: 10.1016/j.biocel.2005.03.006 [PubMed: 15886047]

26. Uygun BE, Stojsih SE, Matthew HWT: Effects of immobilized glycosaminoglycans on the proliferation and differentiation of mesenchymal stem cells. Tissue Eng. Part A. 15, 3499–3512 (2009). doi: 10.1089/ten.TEA.2008.0405 [PubMed: 19456238]

27. Dombrowski C, Song SJ, Chuan P, Lim X, Susanto E, Sawyer AA, Woodruff MA, Hutmacher DW, Nurcombe V, Cool SM: Heparan Sulfate Mediates the Proliferation and Differentiation of Rat Mesenchymal Stem Cells Stem Cells Dev. 18, 661–670 (2009). doi:10.1089/scd.2008.0157 [PubMed: 18690792]

28. Manton KJ, Leong DFM, Cool SM, Nurcombe V: Disruption of heparan and chondroitin sulfate signaling enhances mesenchymal stem cell-derived osteogenic differentiation via bone morphogenetic protein signaling pathways. Stem Cells. 25, 2845–2854 (2007). doi:10.1634/stemcells.2007-0065 [PubMed: 17702986]

29. Celikkin N, Rinoldi C, Costantini M, Trombetta M, Rainer A,   wi szkowski W: Naturally derived proteins and glycosaminoglycan scaffolds for tissue engineering applications. Mater. Sci. Eng. C. 78, 1277–1299 (2017). doi: 10.1016/j.msec.2017.04.016

30. Pfeifer CG, Berner A, Koch M, Krutsch W, Kujat R, Angele P, Nerlich M, Zellner J: Higher ratios of hyaluronic acid enhance chondrogenic differentiation of human MSCs in a hyaluronic acid-gelatin composite scaffold. Materials (Basel). 9, (2016). doi:10.3390/ma9050381

31. Christiansen-Weber T, Noskov A, Cardiff D, Garitaonandia I, Dillberger A, Semechkin A, Gonzalez R, Kern R: Supplementation of specific carbohydrates results in enhanced deposition of chondrogenic-specific matrix during mesenchymal stem cell differentiation. J. Tissue Eng. Regen. Med 12, 1261–1272 (2018). doi:10.1002/term.2658 [PubMed: 29490116]

32. Amann E, Wolff P, Breel E, van Griensven M, Balmayor ER: Hyaluronic acid facilitates chondrogenesis and matrix deposition of human adipose derived mesenchymal stem cells and human chondrocytes co-cultures. Acta Biomater. 52, 130–144 (2017). doi:10.1016/j.actbio.2017.01.064 [PubMed: 28131943]

33. Weyers A, Yang B, Yoon DS, Park J-H, Zhang F, Lee KB, Linhardt RJ: A Structural Analysis of Glycosaminoglycans from Lethal and Nonlethal Breast Cancer Tissues: Toward a Novel Class of Theragnostics for Personalized Medicine in Oncology? Omi. A J. Integr. Biol 16, 79–89 (2012). doi: 10.1089/omi.2011.0102

34. Heiskanen A, Hirvonen T, Salo H, Impola U, Olonen A, Laitinen A, Tiitinen S, Natunen S, Aitio O, Miller-Podraza H, Wuhrer M, Deelder AM, Natunen J, Laine J, Lehenkari P, Saarinen J, Satomaa T, Valmu L: Glycomics of bone marrow-derived mesenchymal stem cells can be used to evaluate their cellular differentiation stage. Glycoconj. J 26, 367–384 (2009). doi: 10.1007/s10719-008-9217-6 [PubMed: 19037724]

35. Hasehira K, Hirabayashi J, Tateno H: Structural and quantitative evidence of α2–6-sialylated N-glycans as markers of the differentiation potential of human mesenchymal stem cells. Glycoconj. J. 34, 797–806 (2017). doi: 10.1007/s10719-016-9699-6 [PubMed: 27314244]

36. Kubaski F, Osago H, Mason RW, Yamaguchi S, Kobayashi H, Tsuchiya M, Orii T, Tomatsu S: Glycosaminoglycans detection methods : Applications of mass spectrometry. Mol. Genet. Metab 120, 67–77 (2017). doi: 10.1016/j.ymgme.2016.09.005 [PubMed: 27746032]

37. Sun X, Li L, Overdier KH, Ammons LA, Douglas IS., Burlew CC, Zhang F, Schmidt EP, Chi L, Linhardt RJ: Analysis of Total Human Urinary Glycosaminoglycan Disaccharides by Liquid Chromatography-Tandem Mass Spectrometry. Anal. Chem 87, 6220–6227 (2015). doi: 10.1021/acs.analchem.5b00913 [PubMed: 26005898]

38. Oguma T, Tomatsu S, Montano AM, Okazaki O: Analytical method for the determination of disaccharides derived from keratan, heparan, and dermatan sulfates in human serum and plasma by high-performance liquid chromatography/turbo ionspray ionization tandem mass spectrometry. Anal. Biochem. 368, 79–86 (2007). doi:10.1016/j.ab.2007.05.016 [PubMed: 17603992]

39. Wang C, Lang Y, Li Q, Jin X, Li G, Yu G: Glycosaminoglycanomic profiling of human milk in different stages of lactation by liquid chromatography-tandem mass spectrometry. Food Chem. 258, 231–236 (2018). doi: 10.1016/j.foodchem.2018.03.076 [PubMed: 29655727]

40. Li G, Li L, Tian F, Zhang L, Xue C, Linhardt RJ: Glycosaminoglycanomics of Cultured Cells Using a Rapid and Sensitive LC-MS/MS Approach. ACS Chem. Biol. 10, 1303–1310 (2015). doi: 10.1021/acschembio.5b00011 [PubMed: 25680304]

41. Liu X, Krishnamoorthy D, Lin L, Xue P, Zhang F, Chi L, Linhardt RJ, Iatridis JC: A method for characterising human intervertebral disc glycosaminoglycan disaccharides using liquid chromatography-mass spectrometry with multiple reaction monitoring. Eur. Cell. Mater. 35, 117–131 (2018). doi: 10.22203/eCM.v035a09 [PubMed: 29469163]

42. Dos Santos F, Andrade PZ, Boura JS, Abecasis MM, da Silva CL, Cabral JMS: Ex vivo expansion of human mesenchymal stem cells: a more effective cell proliferation kinetics and metabolism under hypoxia. J. Cell. Physiol. 223, 27–35 (2010). doi:10.1002/jcp.21987 [PubMed: 20020504]

43. Santhagunam A, Dos Santos F, Madeira C, Salgueiro JB, Cabral JMS: Isolation and ex vivo expansion of synovial mesenchymal stromal cells for cartilage repair. Cytotherapy. 16, 440–453 (2013). doi: 10.1016/j.jcyt.2013.10.010 [PubMed: 24364906]

44. Guneta V, Zhou Z, Tan NS, Sugii S, Wong MTC, Choong C: Recellularization of decellularized adipose tissue-derived stem cells: Role of the cell-secreted extracellular matrix in cellular differentiation. Biomater. Sci. 6, 168–178 (2018). doi:10.1039/c7bm00695k

45. Hoshiba T, Lu H, Kawazoe N, Yamada T, Chen G: Effects of extracellular matrix proteins in chondrocyte-derived matrices on chondrocyte functions. Biotechnol. Prog. 29, 1331–1336 (2013). doi:10.1002/btpr.1780 [PubMed: 23847171]

46. Kaukonen R, Jacquemet G, Hamidi H, Ivaska J: Cell-derived matrices for studying cell proliferation and directional migration in a complex 3D microenvironment. Nat. Protoc. 12, 2376–2390 (2017). doi: 10.1038/nprot.2017.107 [PubMed: 29048422]

47. Ragelle H, Naba A, Larson BL, Zhou F, Priji M, Whittaker CA, Del Rosario A, Langer R, Hynes RO, Anderson DG: Comprehensive proteomic characterization of stem cell-derived extracellular matrices. Biomaterials. 128, 147–159 (2017). doi: 10.1016/j.biomaterials.2017.03.008 [PubMed: 28327460]

48. Knudson CB, Knudson W: Cartilage proteoglycans. Semin. Cell Dev. Biol 12, 69–78 (2001). doi: 10.1007/978-3-319-29568-8_1 [PubMed: 11292372]

49. Roughle PJ: The Structure and Function of Cartilage Proteoglicans. Eur. Cells Mater. 12, 92–101 (2006)

50. Mouw JK, Case ND, Guldberg RE, Plaas AHK, Levenston ME: Variations in matrix composition and GAG fine structure among scaffolds for cartilage tissue engineering. Osteoarthr. Cartil. 13, 828–836 (2005). doi: 10.1016/j.joca.2005.04.020 [PubMed: 16006153]

51. Lauder RM, Huckerby TN, Brown GM, Bayliss MT, Nieduszynski I a: Age-related changes in the sulphation of the chondroitin sulphate linkage region from human articular cartilage aggrecan. Biochem. J. 358, 523–528 (2001). doi: 10.1042/0264-6021:3580523 [PubMed: 11513754]

52. Sharma A, Rees D, Roberts S, Kuiper NJ: A case study: Glycosaminoglycan profiles of autologous chondrocyte implantation (ACI) tissue improve as the tissue matures. Knee. 24, 149–157 (2017). doi: 10.1016/j.knee.2016.10.002 [PubMed: 27773574]
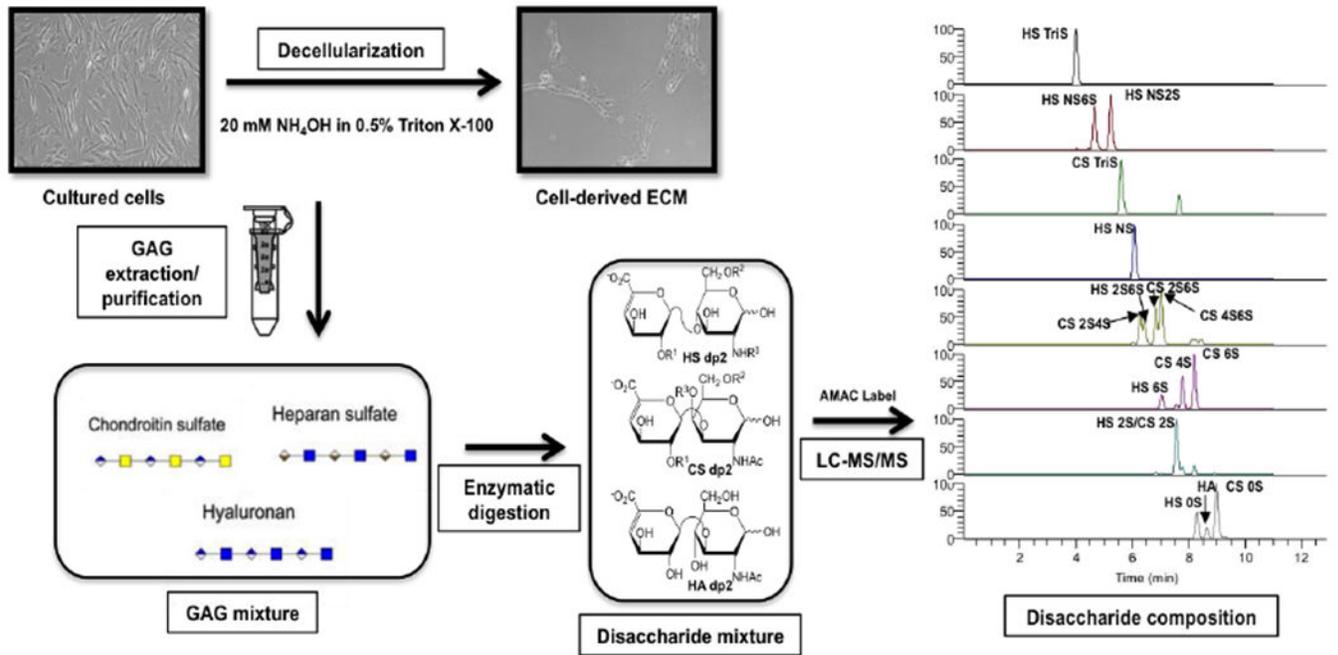
Fig. 1.
Flow chart for cell-derived ECM and respective cultured cell sources sample treatment for GAG disaccharide compositional analysis by LC-MS/MS. GAG were purified from the different cell-derived ECM and respective monolayer cultures and digested by heparinases and chondroitinase ABC, originating a disaccharide mixture. The disaccharide samples were then AMAC-labeled (structures in Supplementary Figure 2) and analyzed by LC-MS/MS MRM to obtain the cell-derived ECM GAG disaccharide composition.
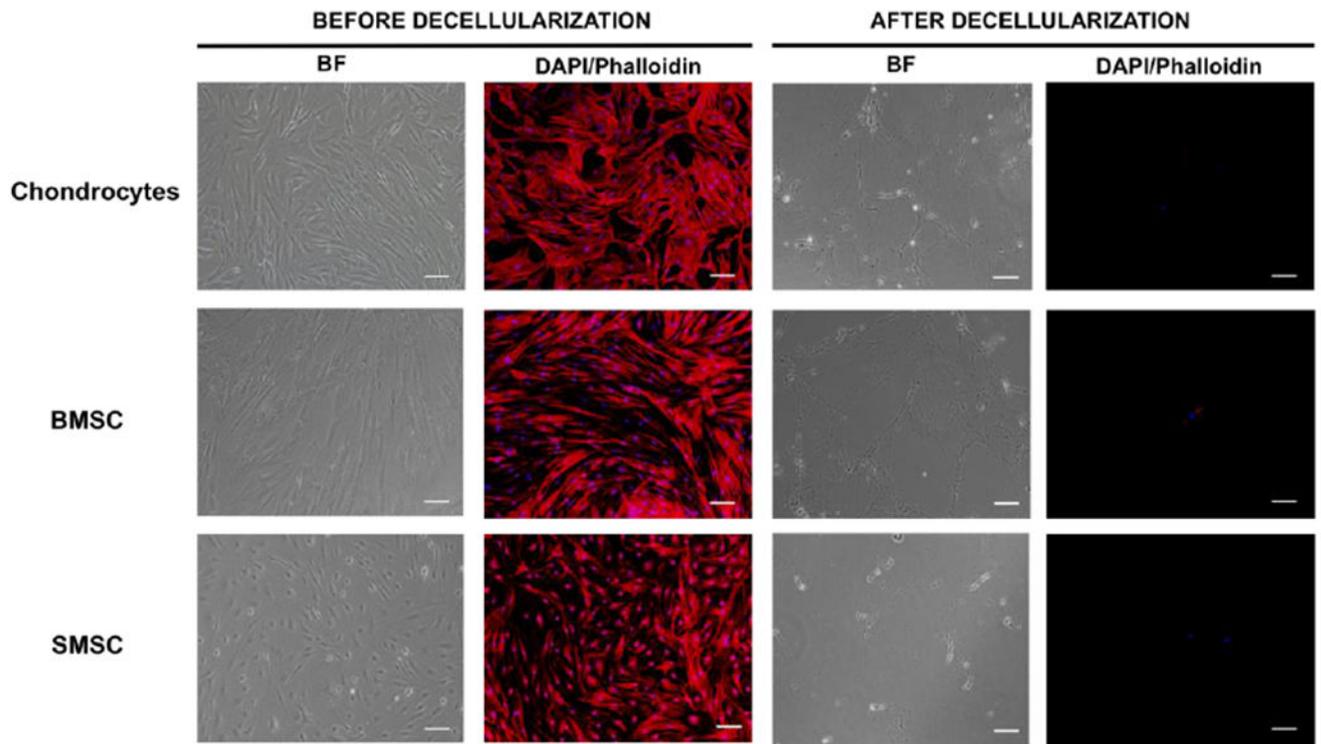
Fig. 2.
Production of decellularized cell-derived ECM from cultures of human chondrocytes, BMSC and SMSC. Phase contrast microscopy and fluorescent microscopy DAPI/phalloidin staining taken in different fields of view before and after the treatment with 20 mM NH_4OH solution with 0.5% Triton X-100 in PBS solution to confirm the success of the decellularization process. DAPI stains cell nuclei blue and phalloidin stains actin-rich cell cytoskeleton red. Scale bar 100 μm.
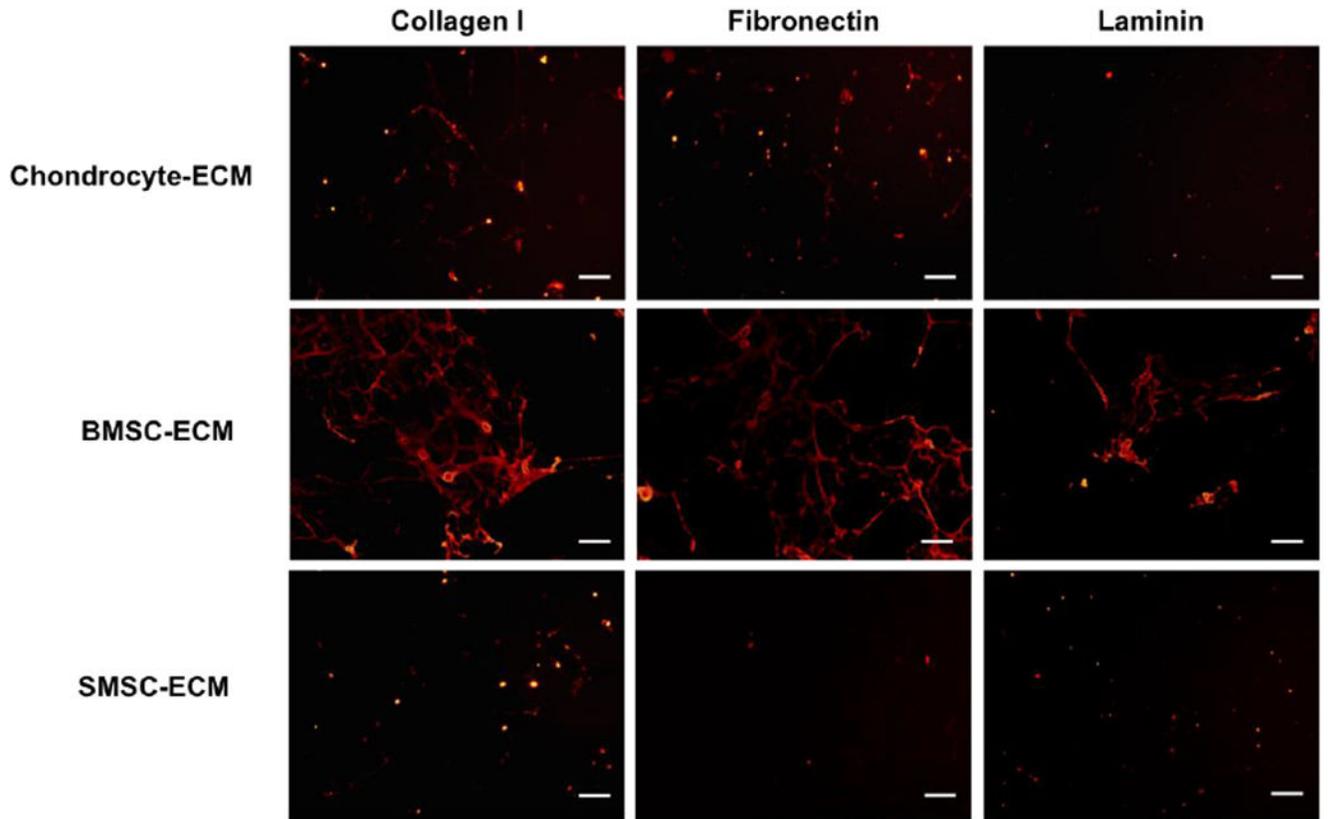
Fig. 3.
Expression of relevant ECM proteins in cell-derived ECM produced from human chondrocytes, BMSC and SMSC. Immunofluorescent staining images of collagen I, fibronectin and laminin showed differences in the abundance and distribution of these proteins in the different types of cell-derived ECM. Scale bar 100 μm.
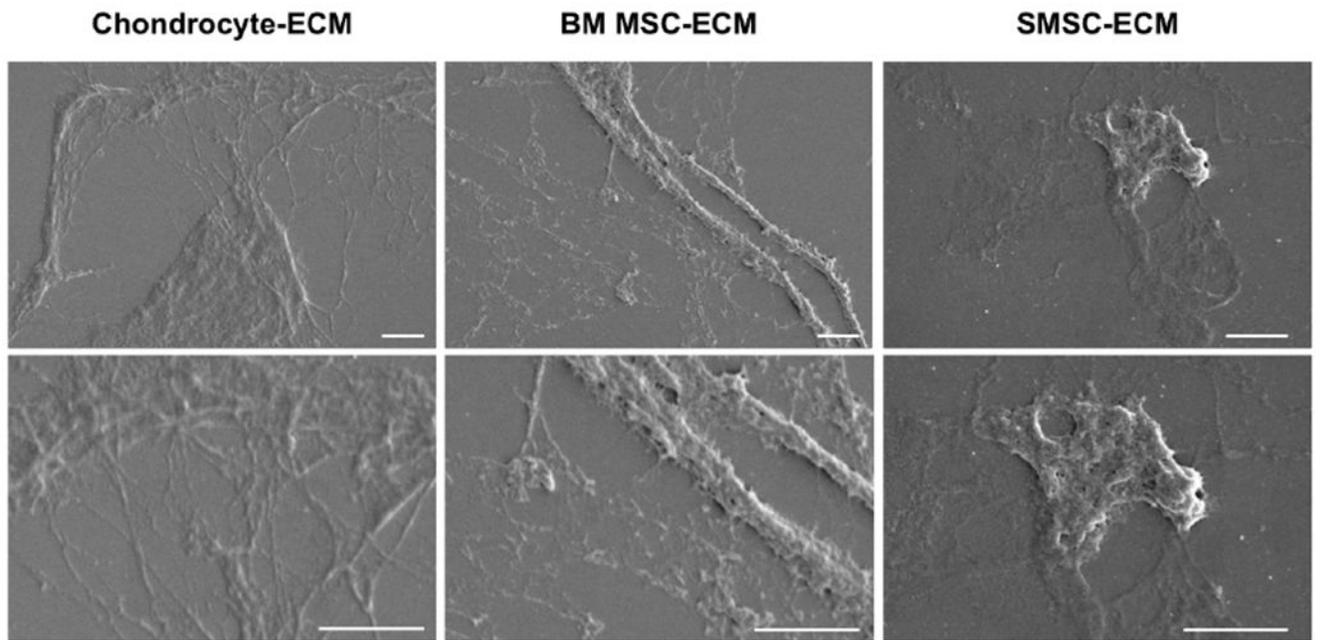
Chondrocyte-ECM   **BM MSC-ECM**   **SMSC-ECM**

Fig. 4.
SEM images of ECM derived from human chondrocytes, BMSC and SMSC after the decellularization protocol. Scale bar 2 μm.
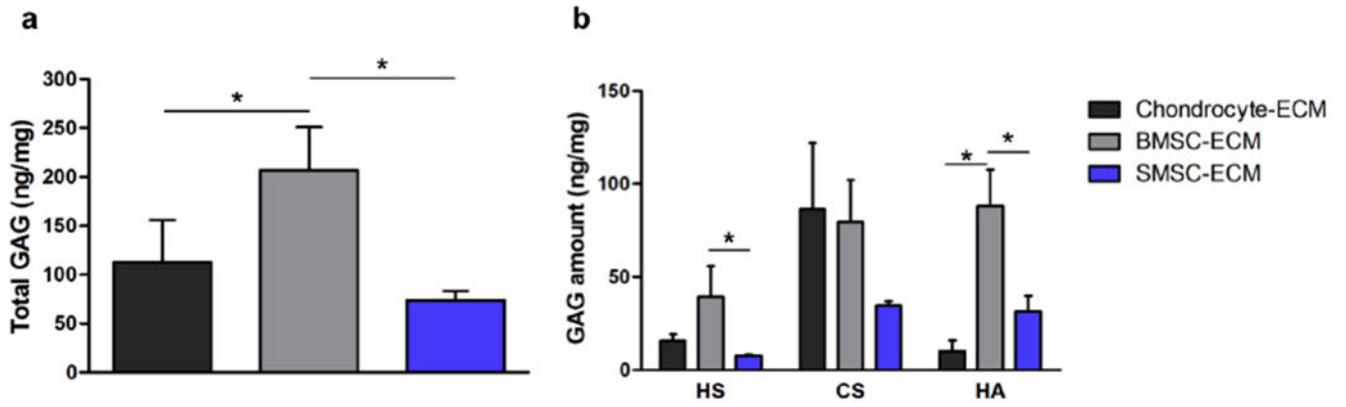
Fig. 5.
GAG composition of the different cell-derived ECM produced from human chondrocytes, BMSC and SMSC. Total GAG (a) and HS, CS, HA total amounts (b) quantified as ng of GAG/mg of dry ECM. Results are presented as mean ± SD of three independent samples (n = 3); *$p < 0.05$.
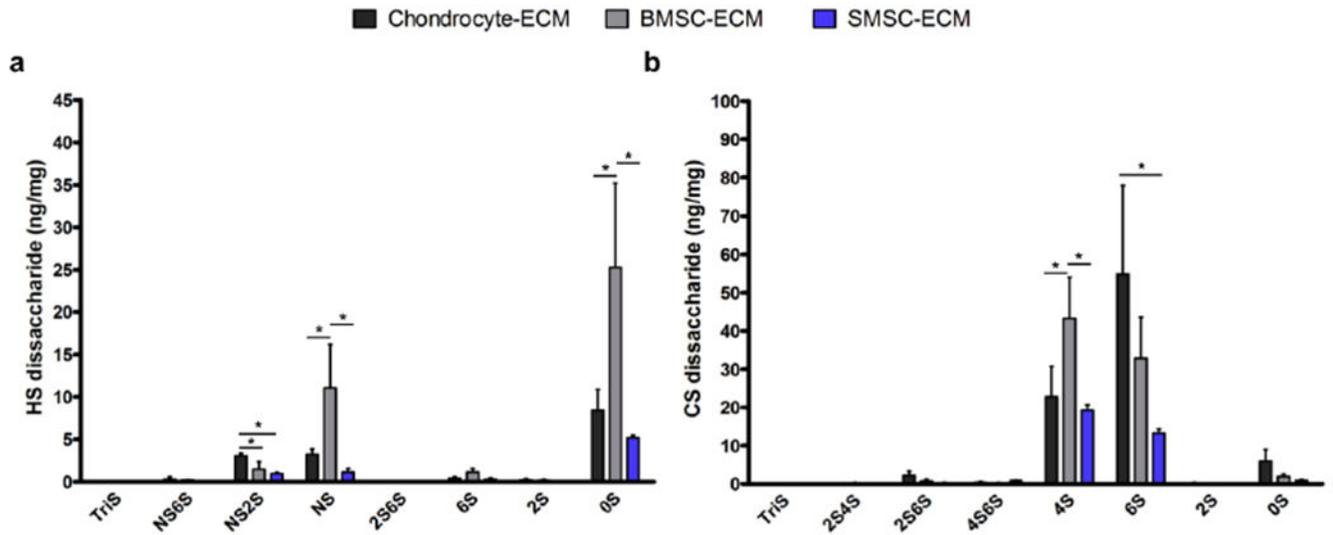
Fig. 6.
HS (a) and CS (b) disaccharide composition of the different cell-derived ECM produced from human chondrocytes, BMSC and SMSC, quantified as ng of GAG/mg of dry ECM. Results are presented as mean ± SD of three independent samples (n = 3); *$p < 0.05$.
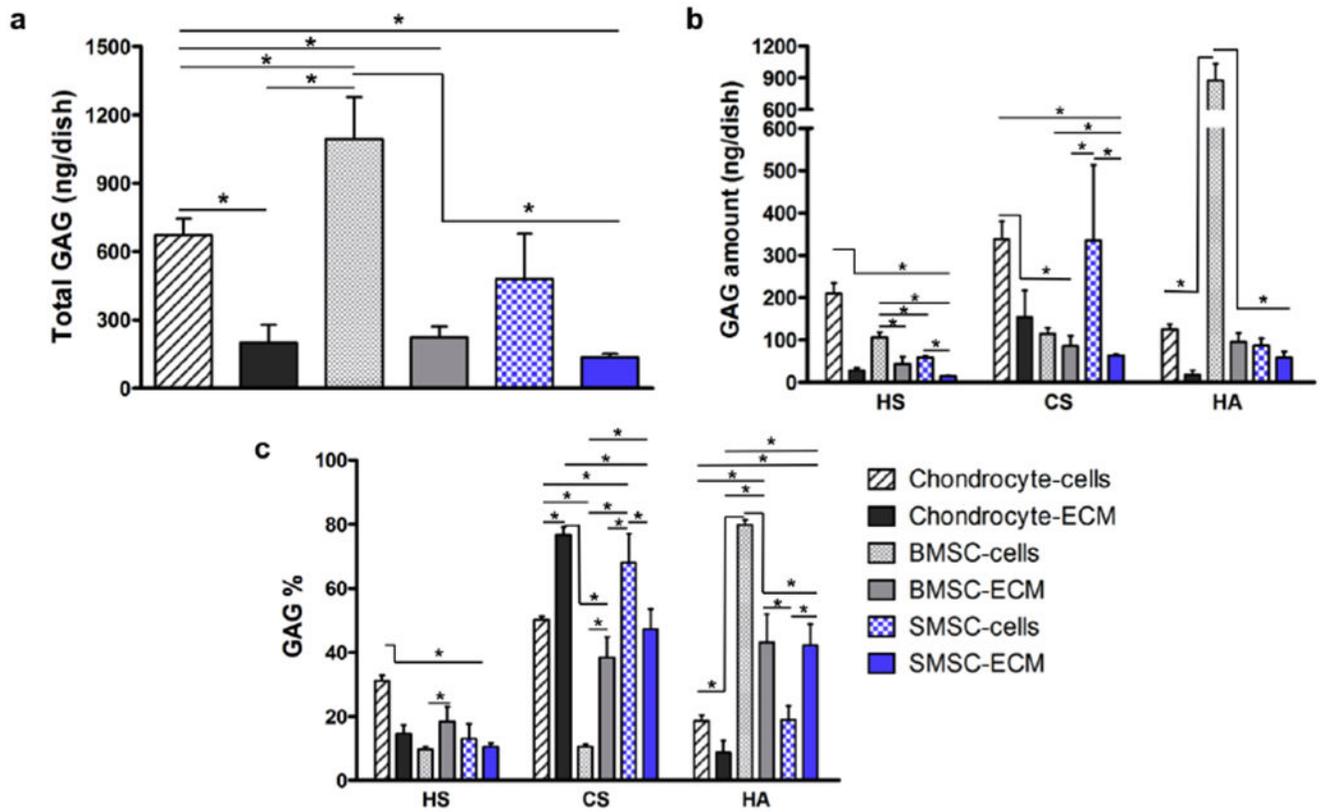
Fig. 7.
Effect of the decellularization protocol on total GAG (a) and HS, CS and HA amounts (b) presented as ng obtained in each culture dish before and after the treatment. Average percentage GAG composition of the different cell-derived ECM and cell culture monolayers (c). Results are presented as mean ± SD of three independent samples (n = 3); *$p < 0.05$.
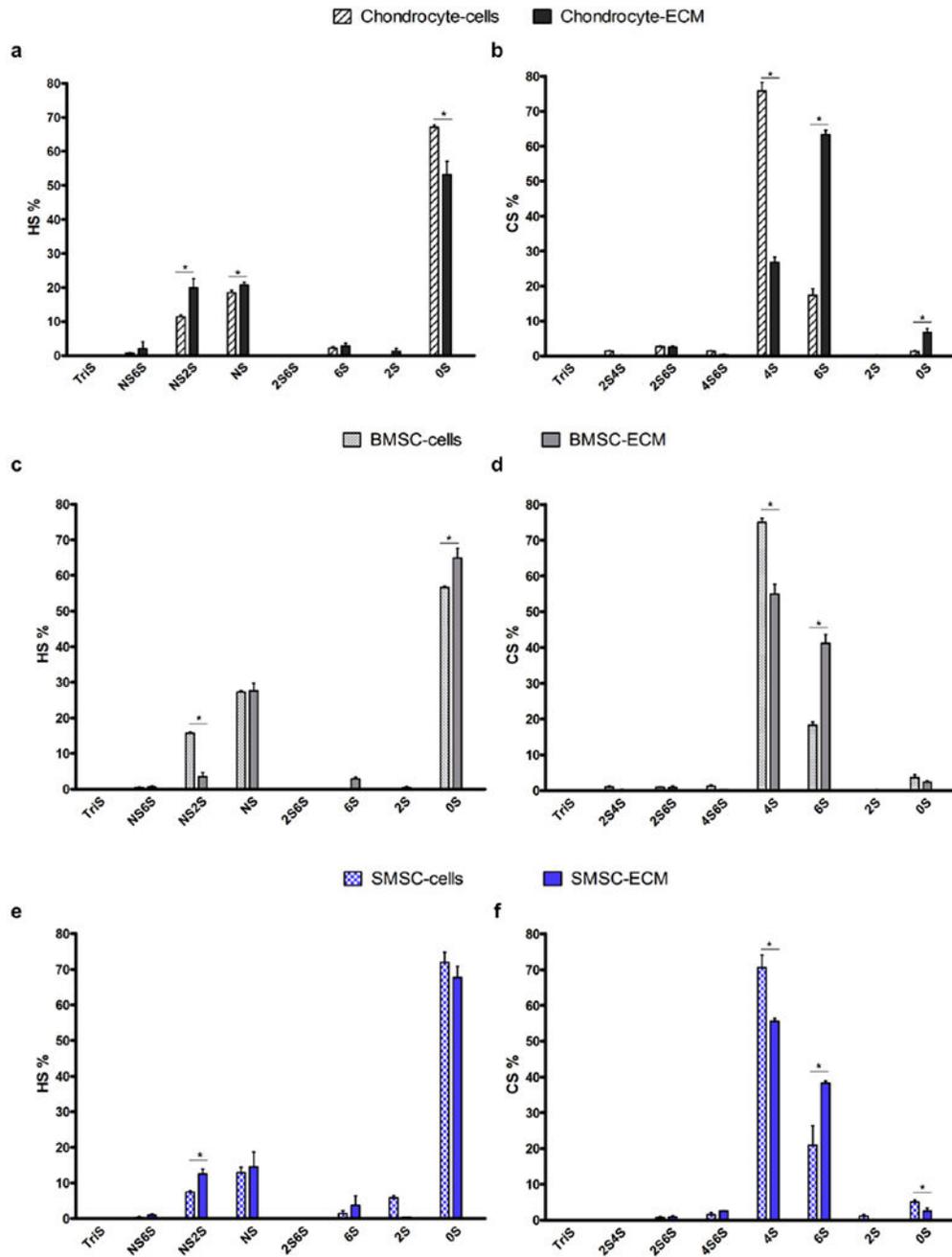
Fig. 8.
Average relative percentage HS (a, c and e) and CS (b, d and f) composition of the different cell-derived ECM and respective cell sources: chondrocytes (a, b), BMSC (c, d) and SMSC (e, f). Results are presented as mean ± SD of three independent samples (n = 3); * $p < 0.05$, denotes significant differences in each HS, CS disaccharide average relative percentage between cell-derived ECM and respective cell source.

Table 1

Heparan sulfate, chondroitin sulfate and hyaluronic acid disaccharide structures. The disaccharide structures in the Table (left) result from different "R" groups of the structures presented (right). These structures correspond to unsaturated uronic acids (UA's), which were AMAC-labeled (AMAC-derivatized disaccharide structures are provided in Supplementary Figure 2), analyzed by LC-MS/MS and used as standards.

HS disaccharides	
$TriS_{HS}$	UA2S(1,4)GlcNS6S
$NS6S_{HS}$	UA (1,4)GlcNS6S
$NS2S_{HS}$	UA2S(1,4)GlcNS
NS_{HS}	UA (1,4)GlcNS
$2S6S_{HS}$	UA2S(1,4)GlcNAc6S
$6S_{HS}$	UA (1,4)GlcNAc6S
$2S_{HS}$	UA2S(1,4)GlcNAc
$0S_{HS}$	UA(1,4)GlcNAc
CS disaccharides	
$TriS_{CS}$	UA2S(1,3)GalNAc4S6S
$2S4S_{CS}$	UA2S(1,3)GalNAc4S
$2S6S_{CS}$	UA2S(1,3)GalNAc6S
$4S6S_{CS}$	UA (1,3)GalNAc4S6S
$2S_{CS}$	UA2S(1,3)GalNAc
$4S_{CS}$	UA (1,3)GalNAc4S
$6S_{CS}$	UA (1,3)GalNAc6S
$0S_{CS}$	UA(1,3)GalNAc
HA disaccharide	
$0S_{HA}$	UA(1,3)GlcNAc

HS disaccharide unit

CS disaccharide unit

HA disaccharide unit